Persistence-Speed Coupling Enhances the Search Efficiency of Migrating Immune Cells

M. Reza Shaebani,[1,2,*] Robin Jose,[1] Ludger Santen,[1,2] Luiza Stankevicins,[3] and Franziska Lautenschläger[2,3,4]
[1]Department of Theoretical Physics, Saarland University, 66123 Saarbrücken, Germany
[2]Center for Biophysics, Saarland University, 66123 Saarbrücken, Germany
[3]INM-Leibniz Institute for New Materials, 66123 Saarbrücken, Germany
[4]Department of Experimental Physics, Saarland University, 66123 Saarbrücken, Germany

(Received 6 May 2020; accepted 4 December 2020; published 28 December 2020)

Migration of immune cells within the human body allows them to fulfill their main function of detecting pathogens. We present experimental evidence showing the optimality of the search strategy of these cells, which is of crucial importance to achieve an efficient immune response. We find that the speed and directional persistence of migrating dendritic cells in our *in vitro* experiments are highly correlated, which enables them to reduce their search time. We introduce theoretically a new class of random search optimization problems by minimizing the mean first-passage time (MFPT) with respect to the strength of the coupling between influential parameters. We derive an analytical expression for the MFPT in a confined geometry and verify that the correlated motion enhances the search efficiency if the mean persistence length is sufficiently shorter than the confinement size. Our correlated search optimization approach provides an efficient searching recipe and predictive power in a broad range of correlated stochastic processes.

DOI: 10.1103/PhysRevLett.125.268102

A successful immune response crucially depends on its first steps: finding harmful pathogens. Migration of immune cells [1–3] is believed to be optimized in the course of evolution to reduce their search time. Adopting an efficient search and navigation strategy has been reported in various biological systems as, for example, in the search for specific target sites over a DNA strand by proteins [4–6], escape through small absorbing boundaries and targeted intracellular transport [7,8], delivery of chemical signals in neurons [9–11], bacterial swimming and chemotaxis [12–15], and animal foraging [16–18]. Nevertheless, the optimality of the search for pathogens and other targets by immune cells has neither been precisely verified nor systematically studied. Understanding the mechanisms of adaptive search and clearance in the immune system opens the way toward more effective cancer immunotherapies and vaccine design. Here, we investigate the dynamics of dendritic cells (responsible for tissue patrolling and antigen capture [3,19]) and present experimental evidence showing that the recently observed universal coupling between their migration speed and directional persistence [20] (mediated by retrograde actin flows) enables them to reduce their search time. Such a persistence-speed coupling was also previously reported for cancer and T cell motility [21,22].

Search and transport efficiency of random processes have been quantified by observables, such as the particle diffusivity [23], transport-limited reactivity [24], and cover time [25,26], or often by the mean first-passage time (MFPT) that a searcher needs to find a target [13,27,28]. Optimal search strategies considered so far minimize the search time with respect to one of the key parameters of the problem, being either a structural property of the environment [7,29] or a parameter of the stochastic motion (e.g., the persistency in active random searches [30], the resetting rate in diffusion processes with stochastic resetting to the initial position [31,32], the ratio between the durations of diffusive and directed motion in intermittent searches [13,33,34], or the speed of the searcher when passing over a target location [16]). However, the influential factors governing the search efficiency are often correlated with each other in reality, necessitating the development of novel strategies for search optimization.

In this Letter, we consider theoretically a correlated stochastic process and introduce, for the first time, a new class of optimal search strategies based on tuning the strength of coupling between key parameters. Inspired by the observed correlations in the dynamics of dendritic cells [20–22], we consider the correlation between the instantaneous migration speed v and local directional persistence p of the searcher. The optimization is achieved by analytically calculating the MFPT and minimizing it with respect to the strength of p-v coupling. The success of the scheme in improving the MFPT nontrivially depends on the ratio between the mean persistence length $\langle \ell_p \rangle$ of the searcher and the system size L; in the regime $\langle \ell_p \rangle \ll L$ ($\langle \ell_p \rangle \sim L$), the correlated motion is advantageous (disadvantageous) for reducing the search time. We validate the analytical predictions with extensive simulations, and the agreement with experimental trends provides an additional support for our model.

Migration of dendritic cells.—To study the dynamics of migrating cells in our *in vitro* experiments, we tracked the

2D motion of murine bone-marrow-derived immature dendritic cells with a typical size of nearly 10 μm. The motion was confined between the cell culture dish and a roof held by microfabricated pillars made out of polydimethylsiloxane as described in Ref. [35] at a height of 3 μm. Both surfaces were coated with PLL-PEG (0.5 mg/ml), a nonadhesive material to exclude movement by cell adhesion. The cell concentration was low enough to treat the cells as noninteracting. Cell nuclei were stained with Hoechst 34580 (200 ng/ml for 30 min) (Sigma Aldrich, St. Louis), and migration was recorded by epifluorescence microscopy for at least 6 h at 37° with a camera of 6.5 μm pixel size and sampling rate of 20 frames per hour.

Experimental results.—A typical cell trajectory is shown in Fig. 1(a), evidencing that the path is more straight when the instantaneous migration speed v is higher. We quantify the local directional persistence—the ability of the cell to maintain its current direction of motion—by $p = \cos\theta$, with θ being the directional change at each recorded position [36–38]. Denoting the distance between two successive recorded positions by d, the local persistence length ℓ_p can be obtained from $p = e^{-d/\ell_p}$ [39–41]. We calculate ℓ_p for each recorded position of each cell trajectory. After averaging the data over small speed bins, a clear coupling between the persistence length and migration speed can be observed, as shown in Fig. 1(b). The behavior can be fitted by a logistic function

$$\ell_p = \frac{\ell_{p_\infty}}{1 + (\ell_{p_\infty}/\ell_{p_o} - 1)e^{-\gamma v}}, \tag{1}$$

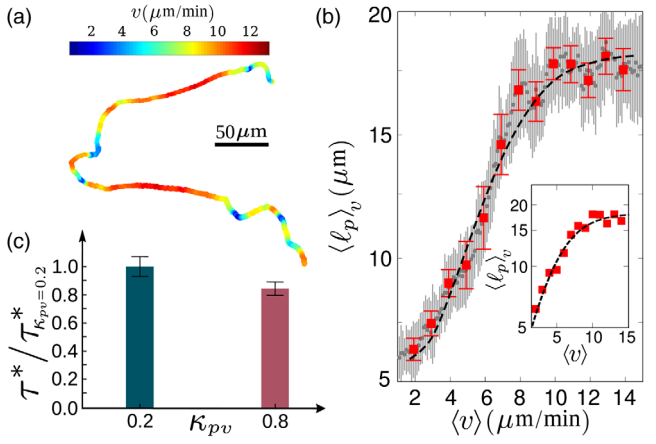

FIG. 1. (a) Sample cell trajectory, color coded with respect to instantaneous migration speed v. (b) Mean persistence length over speed bins, $\langle \ell_p \rangle_v$, versus mean speed in each bin. Red (gray) data represent speed binning intervals of 1.0 (0.1) μm/ min. The dashed line shows the fit via Eq. (1). Inset: Log-lin plot of $\langle \ell_p \rangle_v$ vs $\langle v \rangle$. (c) Comparison between the conditional MFPT τ^* of two categories of cells with low and high p-v correlations but similar mean persistence lengths.

where ℓ_{p_o} and ℓ_{p_∞} represent the initial and saturation levels, respectively, and $\gamma \simeq 0.3$. ℓ_p initially grows exponentially [20] and eventually converges to ℓ_{p_∞} at high speeds. To describe the overall coupling strength for individual cells, we calculate the p-v correlation coefficient $\kappa_{pv} = \{[\mathrm{cov}(p, v)]/(\sigma_p \sigma_v)\}$ for each cell. When calculating κ_{pv} for the averaged data over speed bins of 1 μm/ min shown in Fig. 1(b), a strong correlation $\kappa_{pv} \simeq 0.9$ is obtained.

The key question is whether such a correlated random motion helps the immune cells to improve their search efficiency. To answer this, we select two subpopulations of cells with similar mean persistence lengths 14.6 ± 0.2 μm and 14.3 ± 0.3 μm but distinct mean correlation coefficients 0.2 ± 0.05 and 0.8 ± 0.05, respectively. Using the experimental trajectories, we calculate the conditional (i.e., over successful trials) MFPT τ^*—per unit area for each category and scaled by their mean speeds—to reach a randomly inserted imaginary target of size 1 μm. The search time is nearly 15% lower at higher correlation; see Fig. 1(c). We checked that the observed trend is independent of the target size by varying it by 2 orders of magnitude. In order to understand these MFPT results, we develop a stochastic model for correlated persistent search in the following and prove that the p-v coupling strategy is beneficial only when the mean persistence length is much smaller than the size of the environment, as in the case of dendritic cells.

Correlated persistent search model.—We consider a discrete-time persistent random walk on a two-dimensional square lattice of size L with periodic boundary conditions and an isotropic initial condition for the starting direction of motion [see Fig. 2(a)]. At each time step, the searcher either decides to continue along the previous direction of motion with probability $q + p$ or chooses a new direction, each with a probability q, so that $4q + p = 1$. For a given p, the corresponding persistence length of the walker can be obtained from the probability of changing the direction of motion after ℓ steps as $\ell_p = \sum_{\ell=1}^{\infty} \ell (q+p)^{\ell-1}(1-q-p) = \frac{4}{3}(1/(1-p))$. However, the directional persistence p (and, therefore, ℓ_p) is a variable parameter in our model ranging from 0 (ordinary diffusion) to 1 (ballistic motion), which depends on the instantaneous speed $v(t)$. After updating the orientation, a new speed is drawn from a speed distribution $f(v)$, and the searcher moves accordingly. Note that here we deal with a non-Markovian position process in the presence of memory effects [42,43]. Assuming that a single target of one lattice-unit size is located at $\boldsymbol{r}_T$ (equivalent to regularly spaced targets on an infinite plane with $1/L^2$ density), we introduce $\tau(\boldsymbol{r}, v, \sigma)$ as the MFPT of reaching the target starting at position $\boldsymbol{r}(\neq \boldsymbol{r}_T)$ with arrival direction $\sigma \in \{\rightarrow, \leftarrow, \uparrow, \downarrow\}$ and instantaneous speed v. The evolution of $\tau(\boldsymbol{r}, v, \sigma)$ can be described by the following backward master equation:

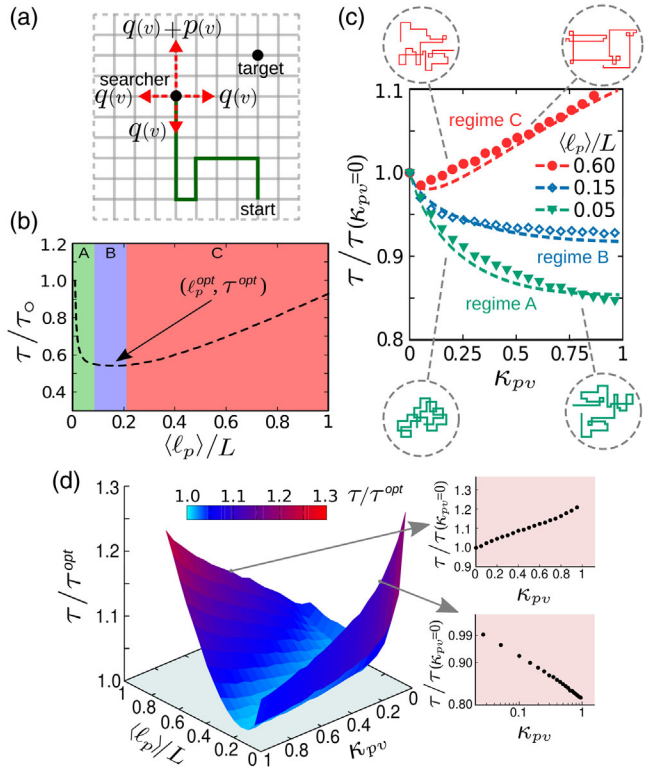

FIG. 2. (a) Sketch of the correlated persistent random search on a square lattice. (b) MFPT τ, obtained from numerical simulations of a constant speed ($\langle v \rangle = 1$) and uncorrelated p-v process, vs ℓ_p normalized by L ($L = 200$). τ is scaled by τ_o of an ordinary random walk; the ratio of their asymptotic diffusion coefficient is $D/D_o = [(1+p)/(1-p)]$. (c) MFPT of a correlated p-v process, scaled by the MFPT of an uncorrelated search (i.e., $\kappa_{pv} = 0$), vs the coupling strength κ_{pv}. Each curve belongs to a different regime of $\langle \ell_p \rangle$ shown in (b). The symbols are simulation results, and the dashed lines represent analytical predictions via Eq. (5) using a persistence extracted from Eq. (6). Insets: Schematics of trajectories with the same $\langle \ell_p \rangle$ but different κ_{pv}. (d) MFPT scaled by the optimal search time of the uncorrelated process vs κ_{pv} and scaled $\langle \ell_p \rangle$. Insets: τ vs κ_{pv} in the extreme regime $\langle \ell_p \rangle \to L$ (top, linear scales) and $\langle \ell_p \rangle \to 0$ (bottom, logarithmic scales).

$$\tau(\boldsymbol{r}, v, \rightarrow) = \int dv' f(v') [(q+p)\tau(\boldsymbol{r} + v\hat{\mathbf{i}}, v', \rightarrow) + q\tau(\boldsymbol{r} - v\hat{\mathbf{i}}, v', \leftarrow) + q\tau(\boldsymbol{r} + v\hat{\mathbf{j}}, v', \uparrow) + q\tau(\boldsymbol{r} - v\hat{\mathbf{j}}, v', \downarrow) + 1], \tag{2}$$

and similar master equations for $\tau(\boldsymbol{r}, v, \leftarrow)$, $\tau(\boldsymbol{r}, v, \uparrow)$, and $\tau(\boldsymbol{r}, v, \downarrow)$. $\{\mathbf{i}, \mathbf{j}\}$ are Cartesian unit vectors. We consider an arrival problem and assume $\tau(\boldsymbol{r}_T, v, \sigma) = 0$ when starting from $\boldsymbol{r} = \boldsymbol{r}_T$. By introducing the Fourier transform $\tau(\boldsymbol{k}, v, \sigma) = \sum_{\boldsymbol{r}} \tau(\boldsymbol{r}, v, \sigma) e^{-i\boldsymbol{k}\cdot\boldsymbol{r}}$ and using $\int dv f(v) \tau(\boldsymbol{k}, v, \sigma) = \tau(\boldsymbol{k}, \sigma)$, after some calculations we obtain

$$\tau(\boldsymbol{k}, \sigma) = \frac{F(k) + S[\delta(\boldsymbol{k}) - e^{-i\boldsymbol{k}\cdot\boldsymbol{r}_T}]}{1 - B_\sigma(k)}, \tag{3}$$

with $k_\sigma \in \{\boldsymbol{k}\cdot\hat{\mathbf{i}}, -\boldsymbol{k}\cdot\hat{\mathbf{i}}, \boldsymbol{k}\cdot\hat{\mathbf{j}}, -\boldsymbol{k}\cdot\hat{\mathbf{j}}\}$, $B_\sigma(k) = \int dv f(v) p(v) e^{ivk_\sigma}$, $F(k) = \int dv f(v) q(v) \sum_\sigma e^{ivk_\sigma} \tau(\boldsymbol{k}, \sigma)$, and $S = L^2$ (see Supplemental Material [44] for details). Next, we multiply Eq. (3) by e^{ivk_σ}, sum over σ, and integrate over v to derive a closed expression:

$$F(k) = \frac{A(k) S[\delta(\boldsymbol{k}) - e^{-i\boldsymbol{k}\cdot\boldsymbol{r}_T}]}{1 - A(k)}. \tag{4}$$

Here, $A(k) = \int dv f(v) p(v) \sum_\sigma [e^{ivk_\sigma}/(1 - B_\sigma(k))]$. Inserting $F(k)$ into Eq. (3) and averaging over all directions σ then yields

$$\tau(\boldsymbol{k}) = \frac{C(k) S[\delta(\boldsymbol{k}) - e^{-i\boldsymbol{k}\cdot\boldsymbol{r}_T}]}{1 - A(k)}, \tag{5}$$

where $C(k) = \frac{1}{4} \sum_\sigma \{[1]/[1 - B_\sigma(k)]\}$. Finally, we apply the inverse Fourier transform (with the components of available modes being $k_i = (2\pi n_i / L)$, $n_i \in [0, L-1]$) and numerically average over all possible starting positions $\boldsymbol{r}$ to obtain the overall MFPT τ.

For an uncorrelated persistent random search with a constant speed, the results of Ref. [30] are recovered (see Supplemental Material [44]). In this case, the MFPT shows a minimum τ^{opt} at an optimal mean persistence length ℓ_p^{opt}; see the simulation results in Fig. 2(b). The scaled optimal value (ℓ_p^{opt}/L) slightly decreases with increasing L in finite systems but saturates in the limit $L \to \infty$. For correlated random searches, we here consider for definiteness a uniform speed distribution with a given mean value $\langle v \rangle$ and a linear correlation between ℓ_p and v, corresponding to an expansion of Eq. (1) up to the first-order term in v. We use

$$\ell_p = \langle \ell_p \rangle + m \kappa_{pv} (v - \langle v \rangle), \tag{6}$$

with κ_{pv} being the strength of persistence-speed coupling ($\kappa_{pv} \in [-1, 1]$) and $m = \langle \ell_p \rangle / \langle v \rangle$. Note that $\langle \ell_p \rangle$ and $\langle v \rangle$ are model parameters which are obtained from linearizing the experimental relation (1). While the local persistence length ℓ_p depends on the choice of the instantaneous speed v, both mean values $\langle v \rangle$ and $\langle \ell_p \rangle$ are kept fixed. By extracting a random $\ell_p(v)$, we calculate the corresponding persistence parameter $p(v) = 1 - \frac{4}{3}[1/\ell_p(v)]$ and insert it in the above formalism to obtain $\tau(\langle \ell_p \rangle, \kappa_{pv})$. We checked that using Eq. (1) instead of Eq. (6) yields qualitatively analogous results to those reported in the following.

Combined effects of $\langle \ell_p \rangle$ and κ_{pv} on search efficiency.—For positive p-v correlations ($0 < \kappa_{pv} \leq 1$), Fig. 2(c) interestingly reveals different dependencies of the MFPT on the coupling strength κ_{pv} for choices of $\langle \ell_p \rangle$ taken from low, intermediate, and high persistence-length regimes A, B, and C, as specified in Fig. 2(b). While τ is a decreasing function of κ_{pv} at low $\langle \ell_p \rangle$, the search efficiency at

high $\langle \ell_p \rangle$ even reduces with increasing κ_{pv}. According to Fig. 2(d), the p-v correlated search strategy is always less efficient than the uncorrelated search with the optimal mean persistence length ℓ_p^{opt}, but the difference decreases as $\langle \ell_p \rangle \to \ell_p^{\mathrm{opt}}$. Nevertheless, adopting the ideal choice $\langle \ell_p \rangle = \ell_p^{\mathrm{opt}}$ is unfeasible in natural systems, because $\langle \ell_p \rangle$ is set by the environmental conditions and the intrinsic structure and dynamics of the real (biological) active agent. Our results reveal that a p-v correlated search strategy provides a realistic search optimization possibility for searchers with $\langle \ell_p \rangle \ll \ell_p^{\mathrm{opt}}$ (regime A), by increasing the chance of long relocations [see the insets in Fig. 2(c)]. As a result, the statistics of reorientations changes toward an optimal combination of long relocations and local tumbling events while keeping the mean persistence length fixed at $\langle \ell_p \rangle$, which enhances the search efficiency. However, in the case of $\langle \ell_p \rangle \gg \ell_p^{\mathrm{opt}}$ (regime C), the trajectory is insufficiently curved, and a positive p-v correlation is even disadvantageous. In the plateau regime B, $\langle \ell_p \rangle$ is around ℓ_p^{opt} and the p-v coupling is less influential. On the contrary, an anticorrelation between persistence and speed ($-1 \leq \kappa_{pv} < 0$) diversifies the reorientation statistics for highly persistent walkers with $\langle \ell_p \rangle \gg \ell_p^{\mathrm{opt}}$, while it homogenizes the relocation sizes in the case of $\langle \ell_p \rangle \ll \ell_p^{\mathrm{opt}}$ and, thus, has a positive effect on regime C but makes the search less efficient in regime A.

For positive p-v correlations and in the extreme persistence-length regime $\langle \ell_p \rangle \to L$, our numerical analysis indicates that τ grows almost linearly with κ_{pv}. On the other hand, τ decays nearly algebraically with κ_{pv} in small persistence-length regime $\langle \ell_p \rangle \to 0$; see the edges of the surface plot in Fig. 2(d) and its insets.

While the above analytical procedure considers uncorrelated successive speeds, we observe a positive speed autocorrelation for migrating dendritic cells in experiments. Thus, in general, one should replace the speed distribution $f(v')$ in the master equation (2) with the probability distribution of speed change $f(v\text{-}v')$, which appears to be analytically intractable. However, our Monte Carlo simulation results (presented in Supplemental Material [44]) verify that the speed autocorrelation plays a relatively insignificant role in determining the search time compared to the influential factors $\langle \ell_p \rangle$ and κ_{pv}.

Simulation results.—In Monte Carlo simulations, we use the *sum-of-uniforms* algorithm [45–47] to generate the desired stochastic motion by correlating the persistence length with the migration speed. The algorithm allows for inducing a certain degree of stochasticity in the resulting ℓ_p values; see the cloud of blue dots in Fig. 3(a). A parameter $\Delta \in [0, 1]$ controls both the fluctuation range of ℓ_p for a given speed and the actual slope of the cloud. Increasing Δ enhances the extent of the cloud and increases its slope (the slope is, however, limited to a given upper threshold $\alpha_{\max}$). This influences the MFPT of a correlated random search as shown in Fig. 3(b), since the actual coupling strength is set

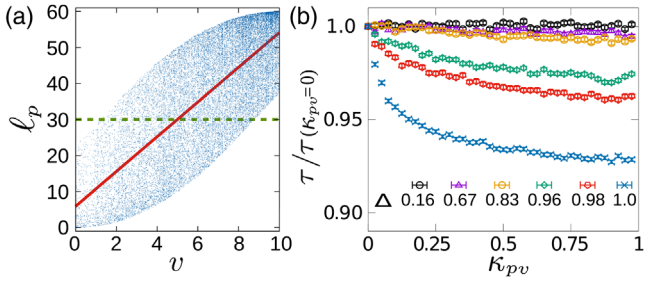

FIG. 3. (a) Example of correlated (v, ℓ_p) pairs generated in simulations with the coupling strength $\kappa_{pv} = 0.8$, drawn from a distribution with $\langle \ell_p \rangle = 30$ (dashed line) and width $\Delta = 1$. The solid line represents the p-v coupling according to Eq. (6). $L = 200$. (b) Influence of the distribution width Δ on the MFPT as a function of the coupling strength κ_{pv}.

by $\Delta \cdot \alpha_{\max} = \Delta \kappa_{pv}$. Nevertheless, in the following, we show the simulation results for $\Delta = 1$; i.e., the slope of the cloud is solely determined by the p-v coupling strength according to Eq. (6). At each time step, we first extract a new ℓ_p according to the above procedure for a given p-v coupling strength κ_{pv} and the current instantaneous speed. Next, a new speed is extracted randomly from a uniform speed distribution with the mean value $\langle v \rangle$ (we checked that an exponential speed distribution with the same mean leads to similar results and the same conclusions). Once the new v and ℓ_p are determined, we extract the instantaneous persistence p of the searcher and move it v substeps within one time step by allowing it to change the direction of motion after each substep according to the persistence probability p.

The analytical predictions for the MFPT in different regimes of $\langle \ell_p \rangle$ obtained via Eq. (5) are compared to simulation results in Fig. 2(c); the agreement is satisfactory despite that ℓ_p is deterministically generated in the analytical procedure, while it is allowed to fluctuate widely around the desired value in simulations; also the possibility of turning during substeps in simulations induces differences. While varying the target size expectedly changes the search time [48,49], it has no clear impact on the efficiency of our correlated scheme when varied over a wide range in our simulations. Another point is that inducing p-v anticorrelation acts in the opposite direction; i.e., it improves the search time in regime C, while it leads to an increased search time in regime A (see Fig. S1 in Supplemental Material [44] for the anticorrelated p-v results and also the modest dependence of the MFPT on the speed autocorrelation).

The fact that the p-v correlation is beneficial for dendritic cells [Fig. 1(c)] suggests that they lie in regime A of relatively small persistence lengths in Fig. 2(b), which is consistent with the natural living environment of immature dendritic cells, i.e., interstitial space of peripheral tissues. For example, the density of the dermal dendritic cells in the skin is about a few hundred cells per mm^2 [50].

Then each dendritic cell patrols, on average, an area of linear size $L \sim 100$ μm when migrating with a persistence length of around 10 μm. Indeed, regime A is even more extended to the right in Fig. 2(b) for such small patrolling areas. The density of dendritic cells in small intrapulmonary airways is even less than a hundred per mm^2 in the absence of inflammation [51]. In such regions, each cell is responsible for patrolling a larger area, and the corresponding $(\langle \ell_p \rangle / L)$ in Fig. 2(b) further shifts to the left in zone A.

In summary, our study suggests improving the search efficiency of active agents by inducing persistence-speed (anti)correlations. The correlated random search is advantageous when moving with a mean persistence length much smaller than the size of the environment (as for dendritic cells in peripheral tissues). In such a case, strengthening the persistence-speed coupling diversifies the reorientation statistics toward an optimal combination of long and short relocations to explore space. On the contrary, the reorientations can be diversified by inducing a persistence-speed anticorrelation for highly persistent active agents, leading to a more efficient search. Our approach offers a fresh insight into the problem of active random searches, with broad applications to other correlated stochastic processes, such as chemotaxis and chemokinesis dynamics, where the environmental and particle properties are connected, in general.

This work was funded by the Deutsche Forschungsgemeinschaft (DFG) through Collaborative Research Center SFB 1027. We thank A. M. Lennon Duménil for support with the dendritic cell system and Raphael Voituriez for discussions.

M. R. S. and R. J. contributed equally to this work. Correspondence and request for materials should be addressed to M. R. S.

*shaebani@lusi.uni-sb.de

[1] T. H. Harris, E. J. Banigan, D. A. Christian, C. Konradt, E. D. Tait Wojno, K. Norose, E. H. Wilson, B. John, W. Weninger, A. D. Luster *et al.*, Nature (London) **486**, 545 (2012).
[2] I. Lavi, M. Piel, A.-M. Lennon-Duménil, R. Voituriez, and N. S. Gov, Nat. Phys. **12**, 1146 (2016).
[3] M. Chabaud, M. L. Heuzé, M. Bretou, P. Vargas, P. Maiuri, P. Solanes, M. Maurin, E. Terriac, M. Le Berre, D. Lankar *et al.*, Nat. Commun. **6**, 7526 (2015).
[4] M. A. Lomholt, T. Ambjörnsson, and R. Metzler, Phys. Rev. Lett. **95**, 260603 (2005).
[5] J. Elf, G.-W. Li, and X. S. Xie, Science **316**, 1191 (2007).
[6] M. Bauer and R. Metzler, Biophys. J. **102**, 2321 (2012).
[7] K. Schwarz, Y. Schröder, B. Qu, M. Hoth, and H. Rieger, Phys. Rev. Lett. **117**, 068101 (2016).
[8] Z. Schuss, A. Singer, and D. Holcman, Proc. Natl. Acad. Sci. U.S.A. **104**, 16098 (2007).
[9] P. C. Bressloff and B. A. Earnshaw, Phys. Rev. E **75**, 041915 (2007).
[10] R. Jose, L. Santen, and M. R. Shaebani, Biophys. J. **115**, 2014 (2018).
[11] S. Fedotov and V. Méndez, Phys. Rev. Lett. **101**, 218102 (2008).
[12] J. Najafi, M. R. Shaebani, T. John, F. Altegoer, G. Bange, and C. Wagner, Sci. Adv. **4**, eaar6425 (2018).
[13] O. Bénichou, C. Loverdo, M. Moreau, and R. Voituriez, Rev. Mod. Phys. **83**, 81 (2011).
[14] G. H. Wadhams and J. P. Armitage, Nat. Rev. Mol. Cell Biol. **5**, 1024 (2004).
[15] E. Perez Ipiña, S. Otte, R. Pontier-Bres, D. Czerucka, and F. Peruani, Nat. Phys. **15**, 610 (2019).
[16] D. Campos, V. Méndez, and F. Bartumeus, Phys. Rev. Lett. **108**, 028102 (2012).
[17] F. Bartumeus and S. A. Levin, Proc. Natl. Acad. Sci. U.S.A. **105**, 19072 (2008).
[18] G. Oshanin, O. Vasilyev, P. L. Krapivsky, and J. Klafter, Proc. Natl. Acad. Sci. U.S.A. **106**, 13696 (2009).
[19] M. L. Heuzé, P. Vargas, M. Chabaud, M. Le Berre, Y.-J. Liu, O. Collin, P. Solanes, R. Voituriez, M. Piel, and A.-M. Lennon-Duménil, Immunological Reviews **256**, 240 (2013).
[20] P. Maiuri, J.-F. Rupprecht, S. Wieser, V. Ruprecht, O. Bénichou, N. Carpi, M. Coppey, S. D. Beco, N. Gov, C.-P. Heisenberg *et al.*, Cell **161**, 374 (2015).
[21] E. R. Jerison and S. R. Quake, eLife **9**, e53933 (2020).
[22] P.-H. Wu, A. Giri, S. X. Sun, and D. Wirtz, Proc. Natl. Acad. Sci. U.S.A. **111**, 3949 (2014).
[23] T. Bertrand, Y. Zhao, O. Bénichou, J. Tailleur, and R. Voituriez, Phys. Rev. Lett. **120**, 198103 (2018).
[24] C. Loverdo, O. Bénichou, M. Moreau, and R. Voituriez, Nat. Phys. **4**, 134 (2008).
[25] M. Chupeau, O. Bénichou, and R. Voituriez, Phys. Rev. E **89**, 062129 (2014).
[26] M. Chupeau, O. Bénichou, and R. Voituriez, Nat. Phys. **11**, 844 (2015).
[27] N. Levernier, J. Textor, O. Bénichou, and R. Voituriez, Phys. Rev. Lett. **124**, 080601 (2020).
[28] S. Redner, *A Guide to First-Passage Processes* (Cambridge University Press, Cambridge, England, 2001).
[29] M. R. Shaebani, R. Jose, C. Sand, and L. Santen, Phys. Rev. E **98**, 042315 (2018).
[30] V. Tejedor, R. Voituriez, and O. Bénichou, Phys. Rev. Lett. **108**, 088103 (2012).
[31] M. R. Evans and S. N. Majumdar, Phys. Rev. Lett. **106**, 160601 (2011).
[32] L. Kusmierz, S. N. Majumdar, S. Sabhapandit, and G. Schehr, Phys. Rev. Lett. **113**, 220602 (2014).
[33] O. Bénichou, M. Coppey, M. Moreau, P.-H. Suet, and R. Voituriez, Phys. Rev. Lett. **94**, 198101 (2005).
[34] C. Loverdo, O. Bénichou, M. Moreau, and R. Voituriez, Phys. Rev. E **80**, 031146 (2009).
[35] M. L. Berre, E. Zlotek-Zlotkiewicz, D. Bonazzi, F. Lautenschlaeger, and M. Piel, Methods Cell Biol. **121**, 213 (2014).
[36] M. R. Shaebani, Z. Sadjadi, I. M. Sokolov, H. Rieger, and L. Santen, Phys. Rev. E **90**, 030701(R) (2014).
[37] Z. Sadjadi, M. R. Shaebani, H. Rieger, and L. Santen, Phys. Rev. E **91**, 062715 (2015).

[38] S. Burov, S. M. A. Tabei, T. Huynh, M. P. Murrell, L. H. Philipson, S. A. Rice, M. L. Gardel, N. F. Scherer, and A. R. Dinner, Proc. Natl. Acad. Sci. U.S.A. **110**, 19689 (2013).
[39] L. D. Landau and E. M. Lifshitz, *Statistical Physics* (Pergamon Press, Oxford, 1958).
[40] M. Doi and S. F. Edwards, *The Theory of Polymer Dynamics* (Oxford University Press, Oxford, 1986).
[41] M. R. Shaebani and Z. Sadjadi, arXiv:1909.05033.
[42] O. Bénichou, T. Guérin, and R. Voituriez, J. Phys. A **48**, 163001 (2015).
[43] T. Guérin, N. Levernier, O. Bénichou, and R. Voituriez, Nature (London) **534**, 356 (2016).
[44] See Supplemental Material at http://link.aps.org/supplemental/10.1103/PhysRevLett.125.268102 for the details of the analytical procedure and the influence of speed auto-correlation on the efficiency of correlated persistent searches.
[45] V. C. Lakhan, J. Stat. Comput. Simul. **12**, 303 (1981).
[46] R. T. Willemain and A. P. Desautels, J. Stat. Comput. Simul. **45**, 23 (1993).
[47] J.-T. Chen, Eur. J. Oper. Res. **167**, 226 (2005).
[48] S. Condamin, O. Bénichou, and M. Moreau, Phys. Rev. Lett. **95**, 260601 (2005).
[49] S. Condamin, O. Bénichou, and M. Moreau, Phys. Rev. E **75**, 021111 (2007).
[50] L. G. Ng, A. Hsu, M. A. Mandell, B. Roediger, C. Hoeller, P. Mrass, A. Iparraguirre, L. L. Cavanagh, J. A. Triccas, S. M. Beverley *et al.*, PLoS Pathogens **4**, e1000222 (2008).
[51] M. A. Schon-Hegrad, J. Oliver, P. G. McMenamin, and P. G. Holt, J. Exp. Med. **173**, 1345 (1991).